Diagn Interv Radiol 2008; 13:177–181

CT and MRI in the evaluation of craniospinal involvement with polyostotic fibrous dysplasia in McCune-Albright syndrome

Nail Bulakbaşı, Uğur Bozlar, İbrahim Karademir, Murat Kocaoğlu, İbrahim Somuncu

ABSTRACT
In this study, the efficacy of computed tomography (CT) and magnetic resonance imaging (MRI) in the evaluation of craniospinal involvement with polyostotic fibrous dysplasia (PFD) in McCune-Albright syndrome (MAS) and related complications were reviewed. In CT, ground-glass appearance with well-defined borders was seen, with medullary widening and cortical thinning. More rarely, cystic/necrotic areas were observed within involved bone. These lesions were seen as hypointense in T1-weighted sequences and as hyperintense in T2-weighted sequences of MRI. There was no heterogeneous contrast enhancement. Cystic/necrotic areas were seen as hyperintense images on T2-weighted sequences. While bone marrow involvement was shown more clearly with MRI, compression of cranial and spinal nerves was determined most effectively by evaluation of CT and MRI together. CT and MRI should be employed together in order to demonstrate the extent of disease, and complications of craniospinal involvement of PFD in patients with MAS.

Key words: • *McCune-Albright syndrome* • *fibrous dysplasia, polyostotic* • *magnetic resonance imaging* • *computed tomography*

From the Department of Radiology (N.B. ✉ *nbulak@gata.edu.tr*), Gülhane Military Medical Academy School of Medicine, Ankara, Turkey.

Received 2 February 2007; revision requested 19 August 2007; revision received 5 September 2007; accepted 25 November 2007.

The syndrome first described by McCune and Albright in 1937 (McCune-Albright syndrome, MAS) classically includes polyostotic fibrous dysplasia (PFD), more than one "café au lait" spot, and endocrine disorders (1–4). While the most common site of involvement is craniofacial (50%), other common sites are (in decreasing order of frequency) the pelvis, the vertebral column, and the shoulders (5). PFD is defined as calcification and ground-glass appearance due to the growth of chondrocytes and fibroblast-like cells, and an increase in non-cellular bone and cartilage-like matrix in regions where osteoblasts are present (1, 2, 4, 5). Despite widespread involvement in PFD, dissemination, proliferation, and exacerbation do not occur in the pubertal period, but existing deformities may progress and lead to progressive neurological abnormalities in patients with craniospinal involvement (5).

Radiologically, there are regular and expansive intramedullary lesions with well-defined borders, which may cause endosteal and cortical thinning (5, 6). Classically three types of computed tomography (CT) images are described as ground glass (56%), homogeneous dense (sclerotic) (23%), and radiolucent (cystic) (21%). These findings are characteristic of fibrous dysplasia (6); however, magnetic resonance imaging (MRI) findings of PFD are variable and may not be as characteristic as CT findings. There is intermediate or low signal intensity in T1-weighted MRI sequences, and intermediate or high signal intensity in T2-weighted MRI sequences. Contrast enhancement is generally heterogeneous with variable intensity (5–11).

In this study, we review the role of CT and MRI in the definition of craniospinal involvement with PFD, and related complications in patients diagnosed with MAS in our hospital between 1996–2007.

Facial and calvarial involvement

There is no preference for a specific bone, but generally facial bones (73%) and the base of the skull (65%) are the most common and the earliest sites of involvement.

Asymmetrical widening of facial bones may contribute to cosmetic impairment and eventually to lion face (leontiasis ossea) (5, 6). This finding is best demonstrated with three-dimensional CT images (Fig. 1). Various dental disorders may be present in the mandible and maxilla (5, 6). Proptosis and hypertelorism may be seen with involvement of the nasal root and orbits (5, 6) (Fig. 2).

Strictures or closures of foramina at the base of the skull may lead to neurological or vascular complications involving the nerves and vessels that pass through these structures. These complications include headache, seizures, cranial nerve anomalies, brain stem compression, spontaneous scalp hemorrhages, atypical infarcts of various types, and local cerebral atrophy (4–6). Stricture of the optic foramen or canal leads

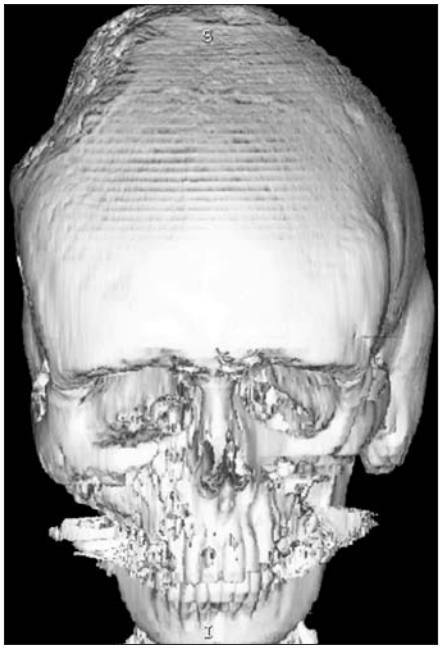

Figure 1. Reconstructed three-dimensional CT image shows lion face appearance due to asymmetrical involvement and enlargement of the bones of the face and the skull.

to progressive loss of vision. In severe cases, increased intracranial pressure may contribute to hypoplastic brain by preventing normal development (Fig. 3). With severe involvement of the occipital bone and the base of the skull, cerebellar tonsils may relocate inferiorly from the foramen magnum due to a decrease in the volume of the posterior fossa that may contribute to acquired Chiari I malformation. In this situation, syringomyelia develops within the spinal canal, and increases neurological abnormalities.

With involvement of the orbits, sphenoid bone, and pituitary fossa, there may be compression of the pituitary gland, optic nerve, optic chiasm, cavernous sinus, other cranial nerves, and internal carotid artery. Compression of these structures results in the most common neurological complications in patients with MAS (Fig. 4).

With involvement of the temporal bone, the osseous labyrinth is preserved, but stenosis of the internal and external acoustic canal may lead to conductive hearing loss (12) (Fig. 5).

Spinal involvement

Spinal involvement is less common, but may lead to severe clinical features (13). Compression of surrounding neurological structures due

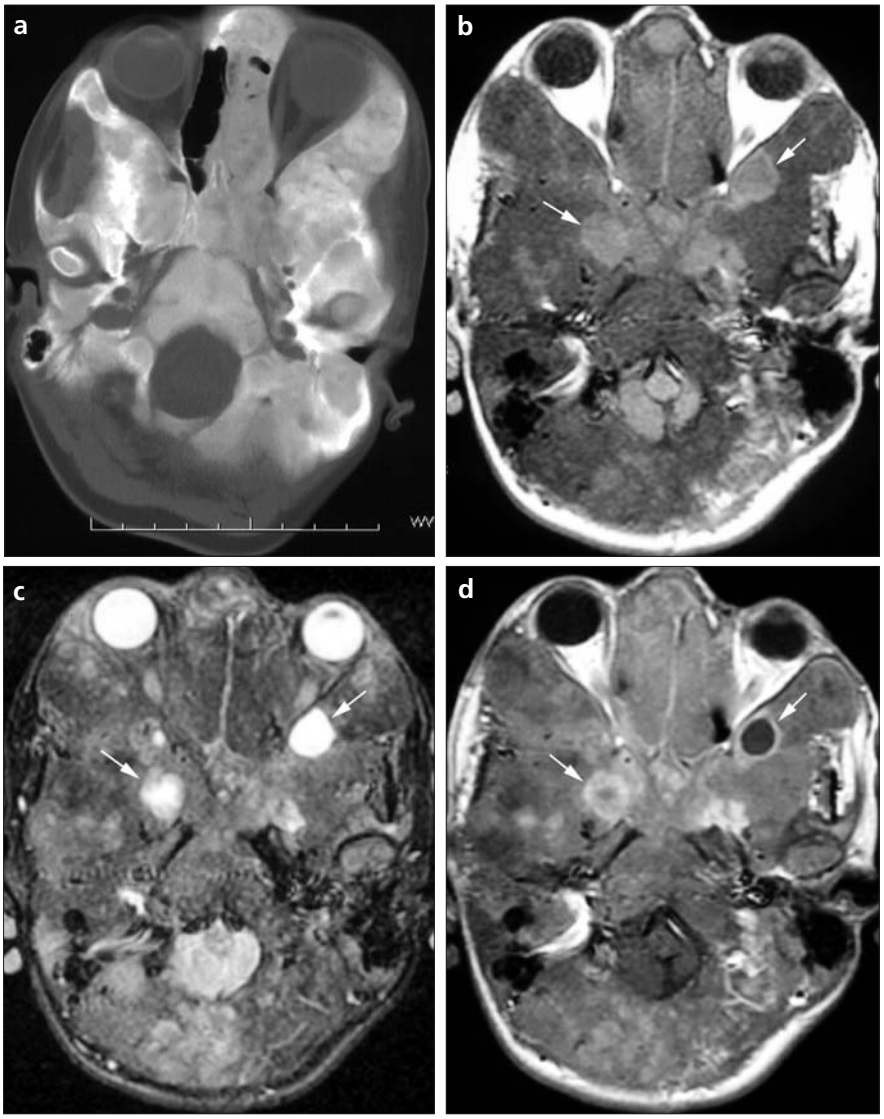

Figure 2. a–d. Axial CT image **(a)**, axial T1-weighted **(b)**, fat-suppressed T2-weighted **(c)**, and post-contrast T1-weighted **(d)** MR images show widespread bone marrow involvement and enlargement of bone structures in the base of the skull and the orbits. There is classical ground-glass appearance on CT **(a)**, but cystic/necrotic areas *(arrows)* are distinguished more clearly on MRI **(b–d)**. Highly cellular regions are more hyperintense **(c)** and show more contrast enhancement than does hypocellular matrix **(d)**. Note that proptosis and hypertelorism are present due to involvement of the orbits and nasal root.

Figure 3. Sagittal T1-weighted MR image demonstrates hypoplasia of the brain, brain stem, and spinal cord due to widespread involvement of the skull.

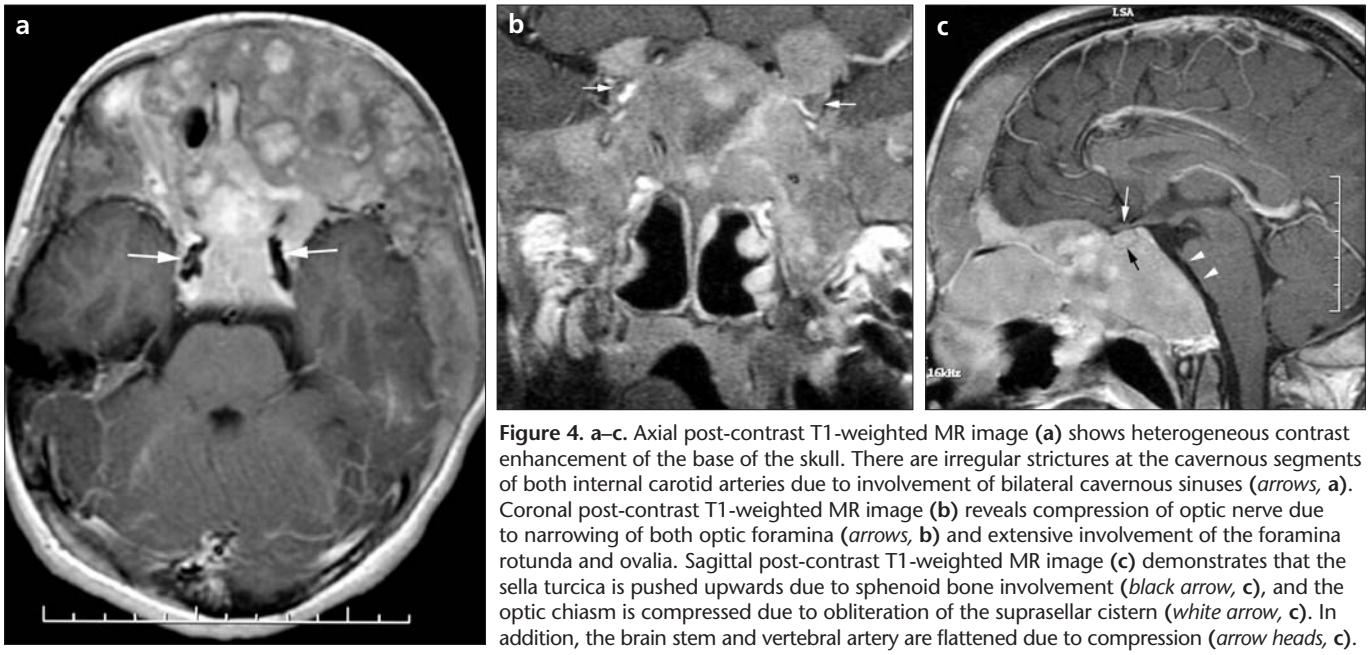

Figure 4. a–c. Axial post-contrast T1-weighted MR image **(a)** shows heterogeneous contrast enhancement of the base of the skull. There are irregular strictures at the cavernous segments of both internal carotid arteries due to involvement of bilateral cavernous sinuses **(***arrows,* **a)**. Coronal post-contrast T1-weighted MR image **(b)** reveals compression of optic nerve due to narrowing of both optic foramina **(***arrows,* **b)** and extensive involvement of the foramina rotunda and ovalia. Sagittal post-contrast T1-weighted MR image **(c)** demonstrates that the sella turcica is pushed upwards due to sphenoid bone involvement **(***black arrow,* **c)**, and the optic chiasm is compressed due to obliteration of the suprasellar cistern **(***white arrow,* **c)**. In addition, the brain stem and vertebral artery are flattened due to compression **(***arrow heads,* **c)**.

Figure 5. Axial CT image through the temporal bone region shows that the involvement of the temporal bones is particularly prominent at left. Preservation of the auditory capsule *(arrows)* with widespread skull-base involvement is seen.

to asymmetrical hyperostotic changes in vertebrae, and enlargement of these bones may lead to progressive neurological abnormalities (Fig. 6). Compression is more prominent in natural anatomical narrow openings such as neural foramina between vertebrae.

Spinal nerve compression syndromes may result from severe kyphoscoliosis, and secondary spinal compression syndromes may result from pathologic fractures of deformed vertebral bodies or posterior elements. The incidence of scoliosis was reported to be between 40% and 52% in patients with PFD (13). Evaluation of CT and MRI findings together provides the most accurate and complete diagnostic information.

Reformation of MRI sequences and three dimensional CT images can provide information to evaluate changes in osseous structures and adjacent tissue. Three dimensional CT images are particularly helpful in patients in whom surgical intervention is planned for cosmetic or functional reasons. While CT is effective in determining cortical changes and expansion, MRI is the modality of choice to show bone marrow changes and compression of surrounding soft tissues. Bone marrow changes that cause ground-glass appearance in CT are shown better on T1- and T2-weighted MRI sequences. While increased fibroblastic activity is seen as hypointense on T1- and T2-weighted sequences, the regions with cystic/necrotic degeneration and increased chondroid matrix cause hyperintense images on the T2-weighted sequences (5–11). The areas that are highly cellular are seen as more hyperintense than the regions that have a paucity of cells and include non-mineralized matrix. These structural differences cause heterogeneous bone marrow appearance and heterogeneous contrast enhancement on T1-weighted images.

Although MRI provides information regarding the extent and complications of the disease (either alone or together with CT), it does not have the same sensitivity for diagnosing PFD as it does for other diseases. Conditions in which an increase in bone marrow in the bones of the base of the skull may lead to expansion or compression, may have similar CT and MRI findings. Such diseases include leukemia, myelofibrosis, polycytemia vera, anemia, myeloproliferative disease such as myelodysplasia syndromes, metastases, non-Hodgkin lymphoma, multiple myeloma, mastocytosis, Paget disease, and histiocytosis X (14–18). In this group of diseases, expansion and ground-glass images may be present in CT, and similar signal changes may be seen on T1- and T2-weighted MRI sequences. The hyperintense spots in images of highly cellular areas, which stand out in contrast to the matrix-rich areas on T1- and T2-weighted images, may be differentiated from the more homogenous involvement of other hematological, myeloproliferative, and myelodysplastic diseases. If the clinical diagnosis is not definitive, the differential diagnosis should include other diseases, and other clinical and laboratory findings should be considered.

In conclusion, MRI and CT are effective modalities to evaluate the extent of PFD, to demonstrate related complications, and to follow up this con-

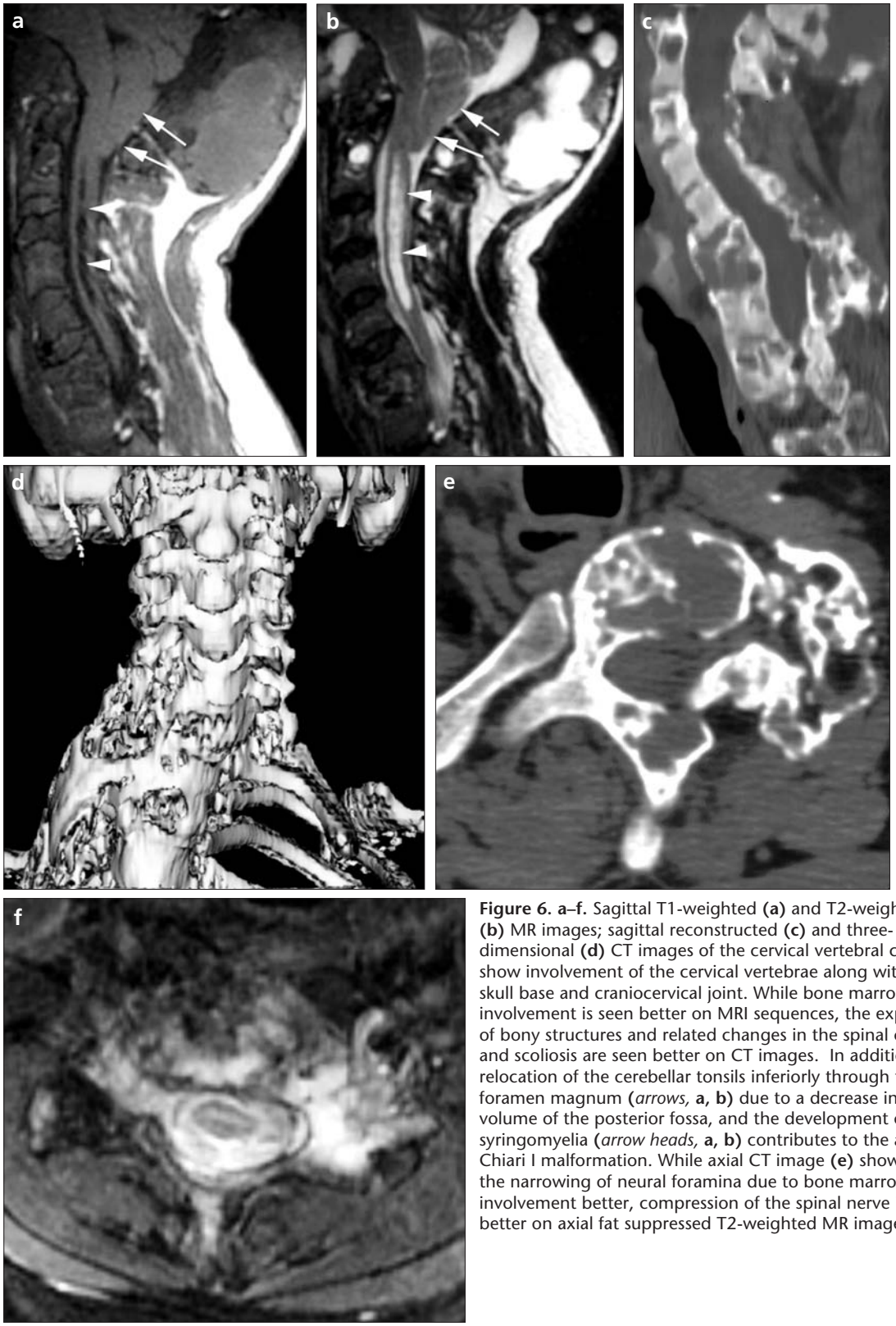

Figure 6. a–f. Sagittal T1-weighted **(a)** and T2-weighted **(b)** MR images; sagittal reconstructed **(c)** and three-dimensional **(d)** CT images of the cervical vertebral column show involvement of the cervical vertebrae along with the skull base and craniocervical joint. While bone marrow involvement is seen better on MRI sequences, the expansion of bony structures and related changes in the spinal canal, and scoliosis are seen better on CT images. In addition, relocation of the cerebellar tonsils inferiorly through the foramen magnum **(***arrows,* **a, b)** due to a decrease in the volume of the posterior fossa, and the development of syringomyelia **(***arrow heads,* **a, b)** contributes to the acquired Chiari I malformation. While axial CT image **(e)** shows the narrowing of neural foramina due to bone marrow involvement better, compression of the spinal nerve is seen better on axial fat suppressed T2-weighted MR image **(f)**.

dition in patients with MAS; however, their diagnostic specificity is limited by the presence of similar features in other diseases. These two modalities should be employed together to evaluate cranial involvement in cases in which the diagnosis is established. The evaluation of MR images from different planes and reformatted CT images together provide a more effective and accurate means to demonstrate the extent of the disease and its neurological complications. Awareness and recognition of different appearances, complications, and accompanying le-

sions of this disease may contribute to accurate diagnosis and appropriate management.

References

1. Albright F, Butler AM, Hampton AO, Smith P. Syndrome characterized by osteitis fibrosa disseminata, areas of pigmentation and endocrine dysfunction, with precocious puberty in females: report of five cases. New Eng J Med 1937; 216:727–746.
2. McCune DJ, Bruch H. Progress in pediatrics: osteodystrophia fibrosa. Am J Dis Child 1937; 54:806–848.
3. Viljoen DL, Versfeld GA, Losken W, Beighton P. Polyostotic fibrous dysplasia with cranial hyperostosis: new entity or most severe form of polyostotic fibrous dysplasia? Am J Med Genet 1988; 29:661–667.
4. De Sanctis C, Lala R, Matarazzo P, et al. McCune-Albright syndrome: a longitudinal clinical study of 32 patients. J Pediatr Endocrinol Metab 1999; 12:817–826.
5. Chong VF, Khoo JB, Fan YF. Fibrous dysplasia involving the base of the skull. AJR Am J Roentgenol 2002; 178:717–720.
6. Fitzpatrick KA, Taljanovic MS, Speer DP, et al. Imaging findings of fibrous dysplasia with histopathologic and intraoperative correlation. AJR Am J Roentgenol 2004; 182:1389–1398.
7. Shah ZK, Peh WC, Koh WL, Shek TW. Magnetic resonance imaging appearances of fibrous dysplasia. Br J Radiol 2005; 78:1104–1115.
8. Jee WH, Choi KH, Choe BY, Park JM, Shinn KS. Fibrous dysplasia: MR imaging characteristics with radiopathologic correlation. AJR Am J Roentgenol 1996; 167:1523–1527.
9. Casselman JW, De Jonge I, Neyt L, De Clercq C, D'Hont G. MRI in craniofacial fibrous dysplasia. Neuroradiology 1993; 35:234–237.
10. Defilippi C, Chiappetta D, Marzari D, Mussa A, Lala R. Image diagnosis in McCune-Albright syndrome. J Pediatr Endocrinol Metab 2006; 19:561–570.
11. Amaral L, Chiurciu M, Almeida JR, Ferreira NF, Mendonca R, Lima SS. MR imaging for evaluation of lesions of the cranial vault: a pictorial essay. Arq Neuropsiquiatr 2003; 61:521–532.
12. Brown EW, Megerian CA, McKenna MJ, Weber A. Fibrous dysplasia of the temporal bone: imaging findings. AJR Am J Roentgenol 1995; 164:679–682.
13. Leet AI, Magur E, Lee JS, Wientroub S, Robey PG, Collins MT. Fibrous dysplasia in the spine: prevalence of lesions and association with scoliosis. J Bone Joint Surg Am 2004; 86:531–537.
14. Roca M, Mota J, Giraldo P, et al. Systemic mastocytosis: MRI of bone marrow involvement. Eur Radiol 1999; 9:1094–1097.
15. Ollivier L, Gerber S, Vanel D, Brisse H, Leclère J. Improving the interpretation of bone marrow imaging in cancer patients. Cancer Imaging 2006; 6:194–198.
16. Ghanem N, Lohrmann C, Engelhardt M, et al. Whole-body MRI in the detection of bone marrow infiltration in patients with plasma cell neoplasms in comparison to the radiological skeletal survey. Eur Radiol 2006; 16:1005–1014.
17. Schmidt GP, Schoenberg SO, Reiser MF, Baur-Melnyk A. Whole-body MR imaging of bone marrow. Eur J Radiol 2005; 55:33–40.
18. Nöbauer I, Uffmann M. Differential diagnosis of focal and diffuse neoplastic diseases of bone marrow in MRI. Eur J Radiol 2005; 55:2–32.